Empirically-transformed linear opinion pools☆

Anthony Garratt [a],[*], Timo Henckel [b],[c], Shaun P. Vahey [a],[c]

[a] *University of Warwick, United Kingdom*
[b] *ANU, Australia*
[c] *CAMA, Australia*

A R T I C L E   I N F O

A B S T R A C T

The linear opinion pool (LOP) produces potentially non-Gaussian combination forecast densities. In this paper, we propose a computationally convenient transformation for the LOP to mirror the non-Gaussianity exhibited by the target variable. Our methodology involves a Smirnov transform to reshape the LOP combination forecasts using the empirical cumulative distribution function. We illustrate our empirically transformed opinion pool (EtLOP) approach with an application examining quarterly real-time forecasts for U.S. inflation evaluated on a sample from 1990:1 to 2020:2. EtLOP improves performance by approximately 10% to 30% in terms of the continuous ranked probability score across forecasting horizons.

© 2022 International Institute of Forecasters. Published by Elsevier B.V. All rights reserved.

1. Introduction

The literature on opinion pooling has extensively examined the accuracy of linear opinion pool (LOP) forecast densities for macroeconomic variables; see the discussion in Rossi (2019). The LOP ensures that the shape of the combination has the scope to be more flexible than the individual forecast densities being combined. Via a variant of the "wisdom of the crowd", non-Gaussian distributional features of the sample can be approximated, even if the individual experts utilise linear and (approximately) Gaussian reduced-form models, such as vector autoregressions (VARs).

In this paper, we propose a new methodology to improve the matching of the LOP to the marginal distribution of the target variable. Our approach involves applying a (modified) Smirnov transform to reshape the

LOP combination forecasts using the empirical cumulative distribution function.

We illustrate our methodology with an example for U.S. inflation. Since we aim to study the scope for performance gains from opinion pools in the presence of misspecification, we consider a VAR model space, with misspecified elliptical errors. Each expert uses a unique VAR to produce "real-time" multi-step-ahead approximately Gaussian forecast densities for U.S. inflation. Jore et al. (2010), Garratt et al. (2011), and Rossi and Sekhposyan (2014) consider closely related density forecasting exercises with many misspecified VAR models.

We compare the combination forecast densities from both the empirically transformed opinion pool (EtLOP) and the equal-weight benchmark LOP using a quarterly evaluation sample from 1990:1 to 2020:2. Relative to the conventional LOP, the EtLOP improves forecast performance by around 10% to 30% in terms of the continuous ranked probability score (CRPS). For longer horizons, the performance gains are somewhat larger than for the one-step-ahead forecasts. Furthermore, the EtLOP forecast densities exhibit greater asymmetry and heteroskedasticity than the benchmark LOP and provide more plausible probabilistic assessments of U.S. inflation events. Hence,

our applied work demonstrates that the EtLOP methodology improves the opinion pool's forecasting performance by mirroring the non-Gaussian characteristics of inflation.

Economically important professional forecasters and policymakers use non-Gaussian forecast densities to communicate risks. For example, individual experts in the Survey of Professional Forecasters report non-Gaussian predictive densities, and the Bank of England has published "fan charts" since 1997 for various macroeconomic variables. Cogley et al. (2005) show that individual VAR specifications produce approximately symmetric forecast densities with stochastic volatility.[1] Arguably then, the mid-2000s default reduced-form macroeconomic forecasting methodology is hard to reconcile with the Bank of England's published forecasts from the perspective of an individual model.[2] An important implication of our study is that a forecaster estimating many misspecified VARs, or running a research team considering many VARs, could match the non-Gaussianity of the target variable by using EtLOP, rather than LOP, in the aggregation step. In effect, the "decision maker" using EtLOP introduces a form of non-Gaussian distributional judgement, which is inconsistent with the Gaussian distribution assumption adopted by each individual expert.

A number of academic studies have explored the scope for individual nonlinear and non-Gaussian time series models to improve forecast performance. Recent contributions include the copula modelling approach of Smith and Vahey (2016), the single-equation quantile regression-based methodology developed by Adrian et al. (2019), and the multimodal joint distribution model of Adrian et al. (2021). In contrast, Carriero et al. (2020) argue that stochastic volatility models accommodate sufficient asymmetries for effective density forecasting in practice. In this study, we remain agnostic on the debate about the best single model to forecast inflation (and other key variables), and instead focus on the scope to improve the accuracy of forecast densities produced from opinion pools, where the experts utilise misspecified linear and (approximately) Gaussian models.

Turning to the extant opinion pooling literature, a number of studies have noted that calibration issues can arise with LOP forecast densities. Even if the individual experts have correctly calibrated exactly Gaussian forecast densities, the LOP combination will not generally be correctly calibrated, even with "optimal weights"; see Ranjan and Gneiting (2010) and Gneiting and Ranjan (2013). In practice, the LOP tends to add diffusion to the combination density.[3] Focusing on the second moment of the conditional densities from the LOP, Ranjan and Gneiting (2010) and Gneiting and Ranjan (2013) propose beta

transforms to reduce the spread. Extensions are explored by Bassetti et al. (2018) and Ganics (2017).

In terms of methodology, our EtLOP approach builds on empirical copula papers by, among others, Deheuvels (1979), Deheuvels (1981), Velásquez-Giraldo et al. (2018), and Coe and Vahey (2020) by fitting marginal distributions with non-parametric methods. Recent macroeconomic applications with semi-parametric copulas utilising non-parametrically fitted empirical cumulative distribution functions (ECDFs) include Smith and Vahey (2016), Karagedikli et al. (2019), Amengual et al. (2020), and Loaiza-Maya and Smith (2020). In contrast, Odendahl (2018) uses a parametric copula to model the multivariate dependence in the aggregate SPF.

Even though we adapt copula methods in our study, the EtLOP approach does not involve fitting the dependence in the combination. This is a natural approach given that the LOP ignores the dependence between experts, with computational advantages for applications involving a large number of experts.

The remainder of this paper is structured as follows. In Section 2, we set out our methodology for empirically transformed opinion pools. In Section 3, we apply our methodology to both a simulated example and the U.S. inflation forecasting application. In the final section, we draw some conclusions.

2. A framework for opinion pooling

In this section, we present the details of our proposal to empirically transform the predictive densities from the LOP. We briefly describe conventional opinion pooling and contrast it with our own approach, before discussing some practical considerations.

2.1. Conventional opinion pooling

In the opinion pooling framework, aggregation by a "decision maker" ignores how the individual experts make predictions. The decision maker only combines out-of-sample forecasts for the target variable. For example, for a one-step-ahead forecast, LOP aggregation gives:

$$p^{LOP}(\pi_\tau) = \sum_{j=1}^{J} w_{j,\tau}\, g(\pi_\tau \mid I_{j,\tau}), \qquad \tau = \underline{\tau}, \dots, \overline{\tau}, \qquad (1)$$

where $g(\pi_\tau \mid I_{j,\tau})$ denotes one-step-ahead forecast densities from expert $j = 1, \dots, J$ for the target variable π_τ (inflation, in our application), conditional on the information set $I_{j,\tau}$. The publication delay in the production of real-time macroeconomic data ensures that this information set contains lagged variables, here assumed to be dated $\tau - 1$ and earlier. The non-negative weights, $w_{j,\tau}$, in this finite mixture sum to unity and potentially change through time in the evaluation sample $\tau = \underline{\tau}, \dots, \overline{\tau}$; see the discussion in, for example, Garratt et al. (2014). Multi-step forecasting (by either direct or iterative methods) and various weighting schemes (including time-varying weights) have been extensively explored in the literature.

---

[1] However, there is greater scope for non-Gaussian forecast densities at longer horizons with iterative forecasts.

[2] Galvao et al. (2021) and Allayioti (2020) find that survey information improves the density forecasting accuracy for a single macroeconomic model and small ensembles of models.

[3] There exists a special case where the LOP is appropriately weighted to select a single "correct" expert. Arguably these conditions never arise in macroeconomic applications with experts using misspecified models subject to "uncertain instabilities".
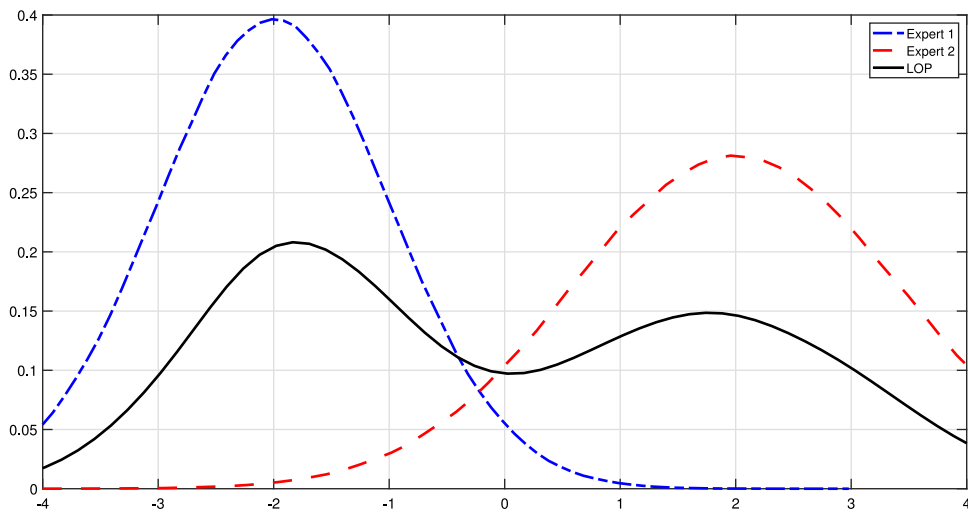
Fig. 1a. LOP and Experts' Density Forecasts.

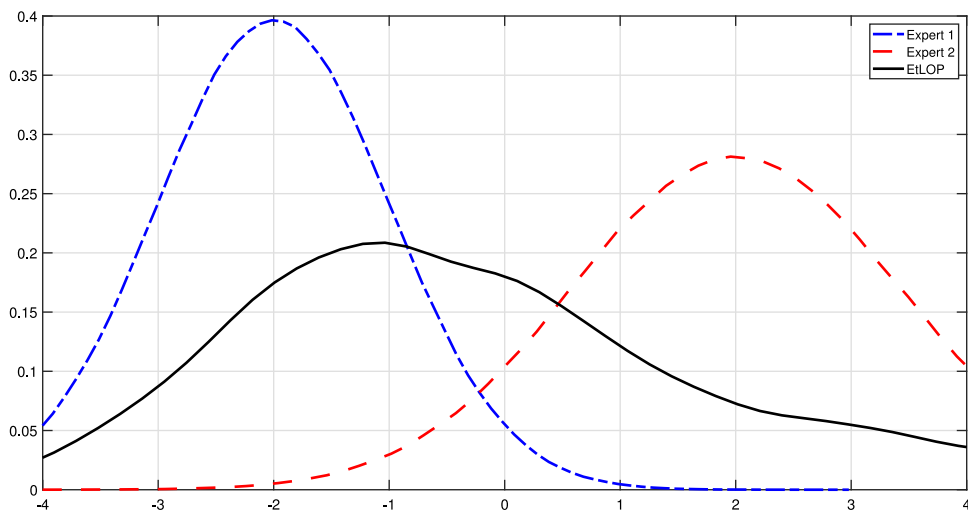**Fig. 1b.** EtLOP and Experts' Density Forecasts.

2.1.1. Illustrative example

An example provided by Kascha and Ravazzolo (2010) helps visually illustrate the capacity for the LOP to introduce non-Gaussianity into the combination density forecast, even with Gaussian experts. The example considers a single observation of the target variable with two experts, where LOP utilises equal-weight aggregation, to mimic the approach of FRB Philadelphia for the Survey of Professional Forecasters (SPF). Figs. 1a and 1b plot the experts' forecasts, where the prediction of Expert 1 (blue, dashed and dotted line) has mean −2.0 and standard deviation 1 and that of Expert 2 (red, dashed line) has mean 2.0 and standard deviation 2.0. Fig. 1a also plots the LOP density (black, solid line), which is bimodal, with a slightly higher peak associated with the forecast mean of Expert 1.

This simple example illustrates several relevant features of conventional opinion pooling with Gaussian experts. First, although the experts' forecast densities are individually Gaussian, the combined LOP density is non-Gaussian. Second, the LOP tends to preserve disagreement across experts about the location of the central probability mass. Hence, the LOP does not inherit the Gaussian distributional characteristics displayed in each expert's forecast. Moreover, this equal-weight LOP, used in practice for the SPF, introduces no information from the history of the target macroeconomic variable (other than as captured in the experts' forecasts).

2.1.2. Discussion

Even though the SPF aggregation by FRB Philadelphia uses equal weights, many studies have examined whether "recursive" and "optimal" weighting improves the LOP's predictive accuracy for macroeconomic data. For example, Geweke and Amisano (2011) argue for optimal combinations based on maximising the Kullback–Leiber information criterion (KLIC), and Jore et al. (2010) report stronger

forecasting performance from LOP with recursively updated weights based on the logarithmic score of each expert. In both cases, the history of the target variable influences the weights.

Nevertheless, the FRB Philadelphia's equal-weight approach has considerable empirical support. In the short samples typical of most macroeconomic density forecasting applications, many studies have noted that equal weights perform as well as more complex weighting schemes. This empirical regularity is sometimes referred to as the "equal-weight puzzle" in both density and point forecasting settings. See, for example, the discussions in Timmermann (2006) and Diebold and Shin (2019).

Even the recursive weights based on relative forecast performance used by (among others) Jore et al. (2010) tend to give little variation across experts in very short samples. As a result, the LOP forecasts with a large number of experts and relatively little disagreement across experts often exhibit approximately Gaussian features.[4]

On the other hand, in long samples of, say, high-frequency financial time series data, recursive weights can result in expert selection, where one expert dominates. In these circumstances, the functional forms of the conventional LOP densities tend to mirror those of the dominant expert. As noted by Geweke and Amisano (2011), optimisation based on the KLIC offers scope to weight experts more evenly, typically generating more complex forecast densities from the LOP as a result. Aastveit et al. (2019) and Rossi (2019) provide discussions of various weighting schemes aimed at improving forecast performance.

Ranjan and Gneiting (2010) and Gneiting and Ranjan (2013) demonstrate that despite "optimal" weights across experts—as constructed by Geweke and Amisano (2011)—and individually well-calibrated experts, the LOP will not typically generate uniformly distributed probability integral transforms (PITs). The LOP aggregation approach tends to amplify the spread of the forecast densities in practice.[5] Gneiting and Ranjan's proposal for the beta linear opinion pool (BLOP) suggests a transformation of the LOP's conditional forecast densities using the beta distribution. In their examples, BLOP is more effective than the optimal-weight LOP, described by Geweke and Amisano (2011), which tends to be overly diffuse.

We stress that our EtLOP methodology is aimed at improving the higher-order moments of the conditional forecast densities. Nevertheless, by matching the non-Gaussianity in the marginal distribution for the target variable, EtLOP also influences the spread of the forecast densities, as we discuss in Section 2.2. Similarly, BLOP offers scope to accommodate simple forms of non-Gaussianity because the beta distribution has two parameters to shape the forecast densities.

2.2. Empirically transformed pooling

Recall that our EtLOP methodology involves reshaping the combination forecast densities from the LOP using a fitted marginal distribution for the target variable. And further recall that our aim is to improve the relative accuracy of the combination forecast. The ECDF provides a convenient choice for the marginal distribution, being a step function that represents the entire history of the observations for the target. By construction, the ECDF is marginally calibrated. But this does not necessarily imply that the PITs of the conditional forecast densities from EtLOP will be uniformly distributed. Among others, Rosenblatt (1952), Diebold et al. (1998), Galbraith and van Norden (2012), and Rossi and Sekhposyan (2019) discuss (what is usually known as "probabilistic") calibration and the relationship to the properties of the PITs.[6]

Given our choice for the marginal distribution of the target variable, $F(\pi_t)$, we reshape the LOP combination density forecast by adapting methods developed for pseudo-random number generation. The Smirnov transform allows a researcher to generate a conditional density forecast with the same distribution as a (stationary) target variable via the inverse ECDF, $F^{-1}(\pi_t)$. The approach is often used to generate pseudo-random numbers from a known but non-parametric distribution. In the empirical copula literature, the transform provides a computationally convenient route for prediction from a non-parametric copula density with non-parametric marginal distributions.[7] Because the inverse of the ECDF is used, the methodology is sometimes referred to as "inverse transform sampling".

The idea behind EtLOP is to use the Smirnov transform, and the target variable's ECDF, to generate a conditional forecast density with the same distribution as the target variable. However, the Smirnov-transform step requires that the LOP forecast densities first be transformed to the $(0,1)$ interval; and the various aggregation issues discussed above imply that the distribution of the LOP is unknown but typically non-Gaussian. We proxy this unknown distribution by using the entire history of LOP forecasts.

For expositional ease, we describe our algorithm for a one-step-ahead forecast case, considering a single candidate LOP combination forecast density, $p^{LOP}(\pi_t)$, for one observation of the target variable, π_t, given the history for the target variable, $\pi_1 \ldots \pi_{t-1}$, and the history of the LOP forecast densities, $p^{LOP}(\pi_1), \ldots, p^{LOP}(\pi_{t-1})$.[8]

We break our EtLOP algorithm into four steps.

1. Construct the proxy empirical CDF, $\phi(\cdot)$, for the LOP forecast density from the history of LOP forecast densities. Computationally, this involves pooling (equal-weight) draws (iterates) from the extant historical ensemble of LOP forecasts.

---

[4] Knüppel and Krüger (2022) propose improving the LOP by removing the disagreement between experts.

[5] Given that parsimonious macroeconomic models tend to produce under-dispersed forecast densities, and therefore over-confident experts, this feature perhaps contributes to the forecasting performance of the SPF with an equal-weight LOP. Diebold et al. (2021) demonstrate that extra diffusion improves forecast performance for eurozone inflation forecasts.

[6] For one-step-ahead forecasts, a well-calibrated density forecast has i.i.d. forecast errors as well as uniformly distributed PITs.

[7] Random number generation for a known parametric distribution utilises a parametric CDF instead of the ECDF.

[8] Our forecasting U.S. inflation application that follows extends consideration to multiple forecast origins and horizons.

2. Convert the candidate LOP forecast density, $p^{LOP}(\pi_t)$, to the unit interval using $\phi(\cdot)$. To achieve this in a computationally convenient manner, we rank draws from $p^{LOP}(\pi_t)$ such that $r_t = R_t/(N+1)$, where R_t denotes the rank of each draw within the historical distribution, ϕ, and N is the total number of draws from that distribution.[9]

3. Fit the ECDF for the target variable, $F(\pi_1, \ldots, \pi_{t-1})$. In practice, there are a number of ways to do this, as we discuss below, but non-parametric methods are a pragmatic choice given the unknown distribution of the target variable.

4. Convert the candidate LOP forecast defined on the unit interval, r_t, to the observed scale using the inverse ECDF, $F^{-1}(\cdot)$, for the target variable. This Smirnov transform involves mapping the ranked draws onto the observed scale of the forecast target variable.

2.2.1. Illustrative example

We illustrate the impact of our EtLOP algorithm by reconsidering the Kascha-Ravazzolo example using two Gaussian experts. Recall that Fig. 1a plots the experts' forecasts as densities, where the prediction of Expert 1 (blue, dashed and dotted line) has mean -2.0 and standard deviation 1 and that of Expert 2 (red, dashed line) has mean 2.0 and standard deviation 2.0. Fig. 1a also plots the equal-weight LOP density (black, solid line), whereas Fig. 1b plots the EtLOP density (black, solid line) resulting from the empirical transformation of the equal-weight LOP density. As indicated in the algorithm description, EtLOP requires the extant histories of the target variable and the LOP forecasts. For illustrative purposes, we used the end-sample objects from our inflation forecasting example to produce the EtLOP density plotted in Fig. 1b.[10]

The EtLOP density forecast displayed in Fig. 1b preserves the unimodality of the individual (Gaussian) densities, with the combination peak relatively close to the forecast mean of Expert 1, with visible asymmetry and a long right tail. This contrasts with the conventional equal-weight LOP forecast density, plotted in Fig. 1a, which is bimodal.

2.2.2. Discussion

Considering the Kascha–Ravazzolo example illustrates the contrast between the EtLOP and LOP approaches to opinion pooling. Although the experts' forecast densities are individually Gaussian, the equal-weight LOP forecast density is non-Gaussian, and the EtLOP suggests that the data do not support bimodality, but do support a degree of asymmetry. Put differently, the LOP preserves the disagreement between experts about the central probability mass, whereas the EtLOP consolidates, with greater probability mass between the two experts' densities. The example also demonstrates the scope for EtLOP to produce

less diffuse forecast densities than LOP. This reflects the marginal calibration of the ECDF for the target variable. Although this does not guarantee probabilistic calibration (in terms of the distribution of the PITs), it often helps in practice.

Throughout our applied work, and in the Kascha–Ravazzolo example above, we use a non-parametric method to fit the ECDF. The non-parametric approach is a pragmatic modelling choice given the unknown distribution of the target variable in practice. We fit the ECDF for the target variable with the SSV locally adaptive kernel density estimator proposed by Shimazaki and Shinomoto (2010).[11] Fig. 2a plots the density for inflation in our full U.S. sample, together with a Gaussian density based on the sample mean and standard deviation. The version corresponding to the ECDF case displays considerable asymmetry and a relatively long right tail. As a rough guide to non-Gaussianity, the Shapiro–Wilk test rejects the null of normality with a *p*-value of zero based on the full sample. We emphasise that in our subsequent application, we follow the standard approach in the "real time" macroeconomic literature, fitting all models and the non-parametric margin to data vintages in the public domain at the forecast origin. As a result, the actual fitted ECDF evolves with the expanding window in the analysis. For illustrative purposes, Fig. 2b displays non-Gaussian densities corresponding to ECDFs fitted to a variety of sub-samples. Since the non-parametrically fitted ECDF is (typically) far from Gaussian for any given window of observations, the EtLOP algorithm adds a limited form of heteroskedasticity to the aggregate forecast density.

Of course, there is scope to restrict the marginal distribution to be Gaussian distributed. We explored this variant in our application and discovered that while the resulting forecast densities were preferred to the benchmark LOP, the non-parametric approach was strongly preferred on our inflation sample.[12]

We emphasise that, as with the (equal-weight, recursive-weight, and optimal-weight) LOP (and BLOP), EtLOP does not estimate the dependence structure between experts. Under the information assumptions of conventional linear opinion pooling, the decision maker assumes that the experts' information sets are conditionally independent; see, for example, the discussion in DeGroot and Mortera (1991).

3. Simulation and application

We now illustrate our approach by exploring a simulation, before turning to our application considering forecasts for U.S. inflation.

3.1. Simulation experiment

In this simulation, we adapt the experiment of Gneiting and Ranjan (2013, Section 4.1) to consider a

---

[9] The denominator avoids boundary issues in the subsequent Smirnov transform.

[10] We describe the non-parametric methods used to fit the ECDF, $F(\cdot)$, below.

[11] Non-parametric kernel fitting used the MATLAB function "ksdensity" in an earlier draft, which gave similar forecast performance.

[12] The EtLOP should perhaps be known as the Gaussian-transformed LOP (GtLOP) in this case.
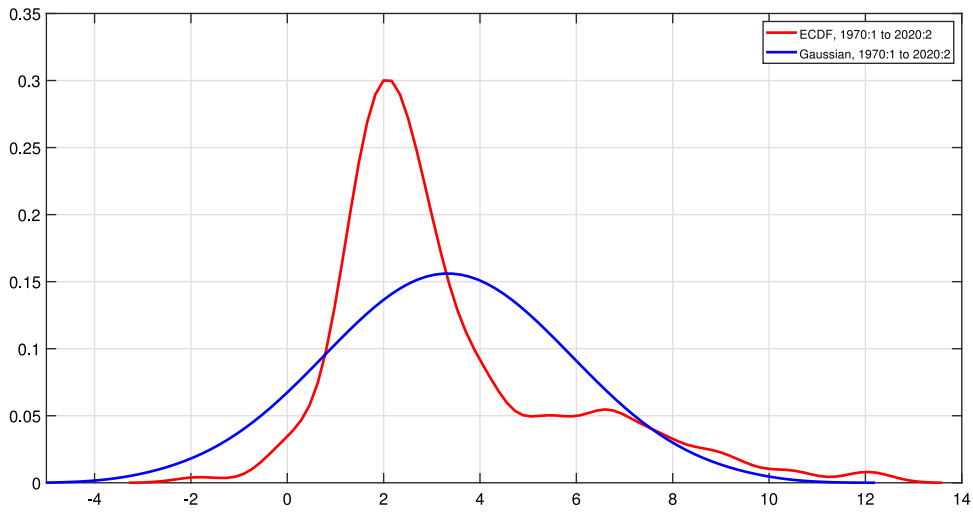
Fig. 2a. Marginal Densities for U.S. Inflation, Full-sample ECDF and Gaussian.
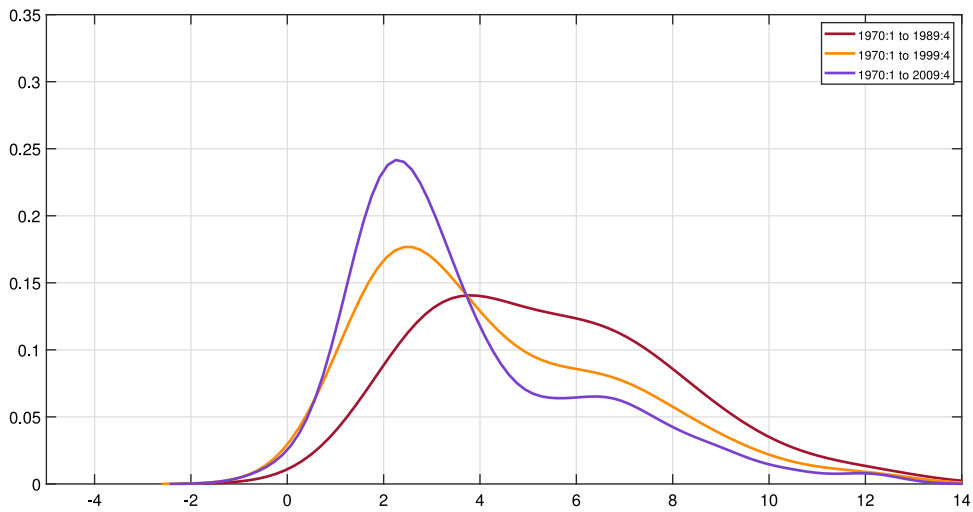

Fig. 2b. Marginal Densities for U.S. Inflation, Sub-sample ECDFs.

non-Gaussian distributed target variable, matching the historical features of U.S. inflation considered in our application. We begin by briefly summarising the baseline Gneiting–Ranjan experiment and then discuss our variation.

3.1.1. Baseline experiment

The Gaussian data generating process (DGP) considered by Gneiting and Ranjan (2013) is:

$$Y = X_0 + a_1 X_1 + a_2 X_2 + a_3 X_3 + \epsilon \qquad (2)$$

where $X_i, i = 0, \dots, 3$ denotes the random and independent variables, a_i denotes the respective parameters, and the disturbance term ϵ is i.i.d. standard normal, $\epsilon \sim \mathcal{N}(0, 1)$. The independent variables are also i.i.d. standard normal.

The three individual experts observe some but not all variables. For example, Expert f_1 observes X_0 and X_1, but

does not observe X_2 and X_3 so that the forecast densities are:

$$f_1 = \mathcal{N}(X_0 + a_1 X_1, 1 + a_2^2 + a_3^2). \qquad (3)$$

Similarly, for the remaining experts:

$$f_2 = \mathcal{N}(X_0 + a_2 X_2, 1 + a_1^2 + a_3^2), \qquad (4)$$

$$f_3 = \mathcal{N}(X_0 + a_3 X_3, 1 + a_1^2 + a_2^2), \qquad (5)$$

where variable X_0 is observed by all experts.

Based on these experts' forecasts, it is straightforward to compute the forecast densities from the LOP (for a variety of weighting schemes) and then to apply EtLOP and BLOP. Following Gneiting and Ranjan (2013), we considered the parameter values $a_1 = a_2 = 1$ and $a_3 = 1.1$, for both a "training" and a "test" sample.

We generated similar results to those reported by Gneiting and Ranjan (2013) for the experts and the LOP

combination using their sample length of 500 observations for both training and test samples. Recall that the purpose of the Gneiting–Ranjan experiment, using a single test sample length of 500 for evaluation, is to examine whether BLOP outperforms optimal-weight and equal-weight LOPs. In terms of relative density forecasting performance as measured by the CRPS, both BLOP and EtLOP gave improvements over the equal-weight LOP. We also found that whereas optimising the LOP weights improved the relative CRPS slightly, the approach did not match BLOP and EtLOP. We emphasise that for applied work with macroeconomic data, the 500 observations considered by Gneiting–Ranjan constitutes a comparatively long sample.[13] Supporting the analysis by Gneiting and Ranjan (2013) of the LOP, we too found that the LOPs, regardless of whether the weights were equal or optimal, produced overly diffuse forecast densities. In contrast, EtLOP and BLOP delivered less diffuse forecast densities.

3.1.2. Experiment with an asymmetrically distributed target variable

With our replication of the Gneiting–Ranjan experiment as background, we now describe our extension to the non-Gaussian distributed variable case.

We began by transforming the target variable from the Gneiting–Ranjan example as follows. First, we non-parametrically fitted the ECDF, $F(\pi_t)$, to our full sample of inflation data exactly as described in Section 2.2.2; see the density plotted in Fig. 2a. Recall that the non-parametrically fitted empirical distribution is considerably more peaked than the Gaussian, and asymmetric with a long right tail; see Figs. 2a and 2b. Second, we ranked the simulated target variable observations, Y, from the baseline (Gaussian) experiment and divided by the number of observations plus one (to avoid boundaries). And third, we used the inverse of the empirical CDF, $F^{-1}(\cdot)$, so that the transformed target variable, denoted $\tilde{Y}$, matched the distribution of the inflation sample—via the Smirnov transform.

We then repeated the Gneiting–Ranjan experiment, with the same experts' parameters, but using the asymmetrically distributed target variable, $\tilde{Y}$, rather than Y, again considering a "training" sample, with the marginal distribution fitted to the same training sample to limit overfitting. Unlike Gneiting and Ranjan (2013), we repeated the test exercise 2000 times for each sample length, and considered sample lengths of 100, 150, 200, 250, and 500.

Fig. 3 plots the (kernel-smoothed) densities of the EtLOP's sample averaged CRPS, based on the 2000 test samples, for simulation sample lengths of 100, 150, 200, 250, and 500.[14] The x-axis displays the CRPS ratio, measuring relative forecast performance for EtLOP, where values of less than one indicate an improvement on the equal-weight benchmark LOP.

There are two striking features from our simulations with a non-Gaussian target variable. First, regardless of which sample length we consider, the EtLOP is never inferior to the benchmark LOP in terms of the CRPS. Second, the relative CRPS plots indicate that forecast performance is robust to sample size, with little variation in the central location of the CRPS densities across sample lengths. However, for smaller samples, the performance gain varies more across simulated samples, but where the central probability mass indicates a considerable expected gain of around 10% to 15%.[15]

As noted in Section 2.1.2, Gneiting and Ranjan (2013) propose the BLOP to correct the second moment of the optimal-weight LOP forecast densities, but this methodology also has some potential to accommodate departures from Gaussianity. Accordingly, we replicated our simulation with BLOP and compared the CRPS results with EtLOP and the equal-weight benchmark LOP. The BLOP failed to match the forecast performance of EtLOP and, for small samples, had approximately similar performance to the equal-weight benchmark LOP. We provide CRPS analysis for the BLOP in the online appendix.

We emphasise that the experts in our experiment make two types of specification errors. First, each expert believes that the target variable has a Gaussian distribution. Second, each expert observes some common information and some expert-specific private information, but does not know the true dependence structure for the target variable. In contrast, the decision maker using opinion pooling believes (correctly) that the target variable is non-Gaussian but does not know the functional form. And following the conventional approach in linear opinion pooling, the decision maker ignores the dependence in the experts' forecasts. This structure for the specification errors is mirrored in the application that follows. The original Gneiting–Ranjan experiment, as noted above, considered a Gaussian-distributed target variable.

3.2. Application: Forecasting U.S. inflation

Given the relatively disappointing forecasting performance of the optimal-weight LOP and BLOP in our simulations with an asymmetric distributed target variable, we report results comparing the EtLOP with an equal-weight benchmark LOP (adopted by FRB Philadelphia for the SPF). The target dates for the quarterly U.S. inflation application run from 1990:1 to 2020:2. As further aids to gauge the relative forecasting performance of EtLOP, we report results for BLOP in the online appendix accompanying this paper, together with those from a univariate unobserved components stochastic volatility (UCSV) model for inflation, estimated by Bayesian methods.

---

[13] On the simulation training data, optimisation gave LOP weight values close to those reported by Gneiting and Ranjan (2013).

[14] We compute the CRPS using Eq. (13) in Gneiting and Ranjan (2011). Suppose the density forecast is f and π_τ is realised inflation we use to evaluate the forecast. Then we define the CRPS as:

$$CRPS(f, \pi_\tau) = E\left[|Z - \pi_\tau|\right] - 0.5E\left[\left|Z - Z^*\right|\right]$$

where Z and Z^* are independent random variables with common sampling density f, i.e. the iterates from the inflation forecast densities and a random permutation of these iterates, respectively.
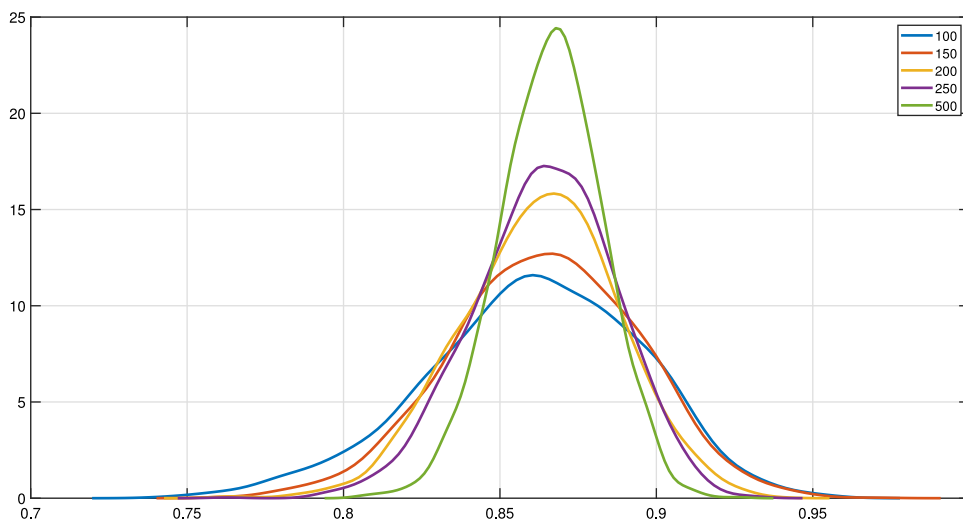
[15] We repeated the analysis using the sample averaged logarithmic score and found similar performance gains for EtLOP across our range of sample sizes.

Fig. 3. EtLOPs Relative CRPS Performance Simulation, by Sample Size.

3.2.1. Experts' models

Each expert utilises a (unique) bivariate VAR model space for inflation, π_t, and the output gap (the deviation of real output from potential), ψ_t. The standard theory that aggregate demand, captured by the output gap, influences the movements in inflation (with unknown time lags), provides some foundation for the empirical specification.

Since we aim to study the scope for performance gains from opinion pools in the presence of misspecification, each expert's VAR is misspecified with elliptical errors.

The jth VAR model takes the form:

$$\begin{bmatrix} \pi_t \\ \psi_t^j \end{bmatrix} = \begin{bmatrix} a_{\pi\pi}^j & a_{\pi\psi}^j \\ a_{\psi\pi}^j & a_{\psi\psi}^j \end{bmatrix} \begin{bmatrix} \pi_{t-1} \\ \psi_{t-1}^j \end{bmatrix} + \begin{bmatrix} \epsilon_{\pi t}^j \\ \epsilon_{\psi t}^j \end{bmatrix},$$
$$t = 1, \ldots, T, \tag{6}$$

where $[\epsilon_{\pi t}^j, \epsilon_{\psi t}^j]' \sim i.i.d. \ N(\mathbf{0}, \mathbf{\Sigma}^j)$. That is, we consider a baseline VAR specification in which the output gap measure has been varied to give J linear and Gaussian VAR models, indexed $j = 1, \ldots, J$. For expositional ease, we ignore the intercept and restrict the lag order of the J VARs to one. Following Garratt et al. (2011), our VAR model space uses seven output gap measures derived from the set of univariate off-model filters considered by Orphanides and van Norden (2002, 2005).

We define the output gap as the difference between observed output and unobserved potential (or the trend component of) output. We denote the (logarithm of) real output in t as q_t, and let μ_t^j be its trend, using definition j, where $j = 1, \ldots, J$. The output gap, ψ_t^j, is therefore defined as the difference between actual output and its jth trend measure at time t. We assume the following linear trend-cycle decomposition:

$$q_t = \mu_t^j + \psi_t^j. \tag{7}$$

The seven methods of univariate trend extraction in our VAR model space are: quadratic, Hodrick–Prescott (HP), forecast-augmented HP, Christiano and Fitzgerald,

Baxter–King, Beveridge–Nelson, and unobserved components. We describe these seven well-known univariate filters in Appendix A.

In our application, we vary a single auxiliary assumption to generate the expert (model) space. Specifically, we vary the lag length in the VAR.[16] If we have J output gap measures, and for any given ψ_t^j we have L variants defined by different values of the maximum lag length, then in total we have $J \times L$ models, each with a corresponding forecast of inflation (and the output gap) from the VAR model space. We restrict L to a maximum of four and therefore we consider 7×4 models—28 forecasts from the experts to be combined.

Although the motivation for deploying these models stems from their common usage by central banks around the world, Orphanides and van Norden (2005) note indifferent real-time out-of-sample forecasting performance for individual VAR models. In contrast, Garratt et al. (2014) note that LOPs of VARs provide competitive real-time density forecasting performance, albeit not as accurate as the univariate UCSV model for U.S. inflation.

3.2.2. Data considerations

Orphanides and van Norden (2002, 2005) stress that output gap measures are subject to considerable data revisions. Failing to account for this by using heavily revised data masks real-time predictive content. Since we are interested in real-time prediction, parameter estimation is recursive for all specifications. Each recursion uses a different vintage of data, where a vintage of data is the vector of time series observations available from a data agency at the forecast origin.

The quarterly real-time real gross domestic product (GDP) U.S. dataset has 124 vintages, with the first vintage dated 1990:1 and the last 2020:4. The raw data for GDP (in practice, gross national product, GNP, for some vintages) are taken from the Federal Reserve Bank of

---

[16] For ease of exposition, we fixed this at one in Eq. (6).
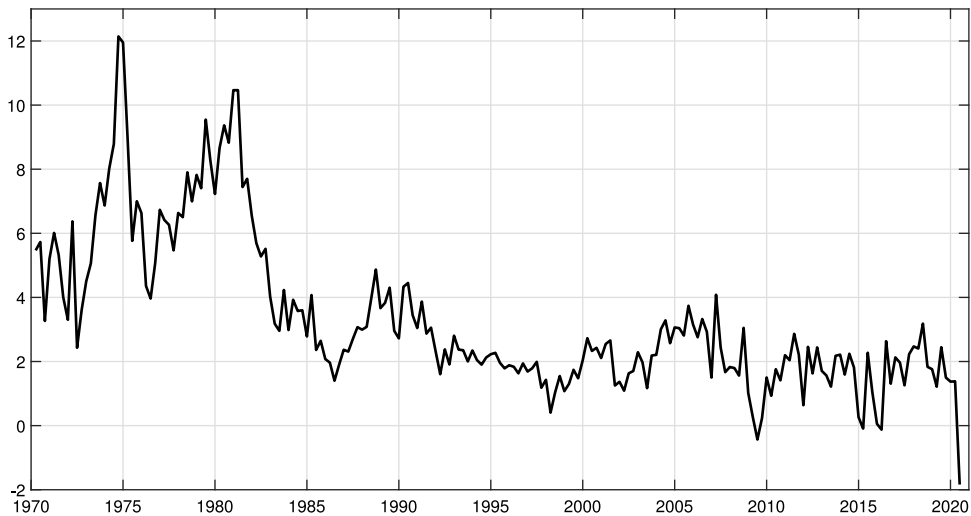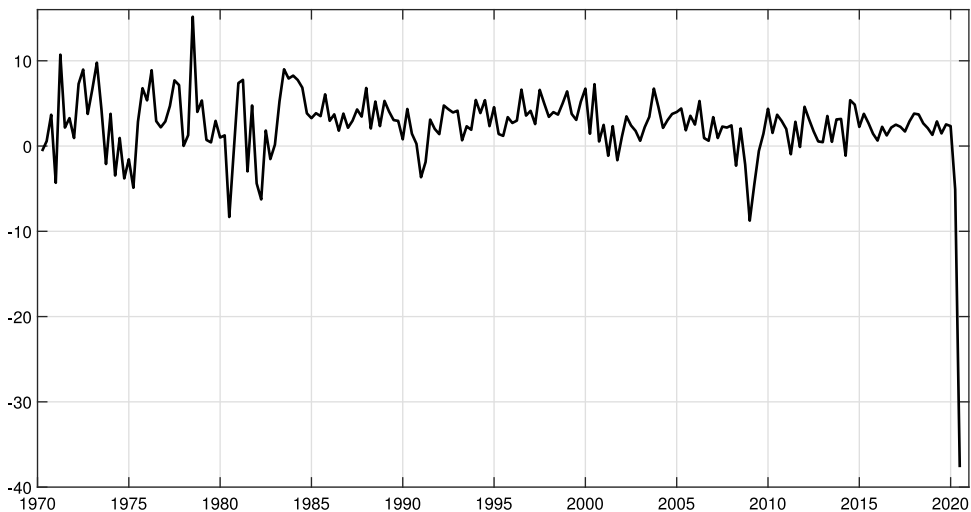
Fig. 4a. U.S. Inflation, 1970:1 to 2020:2.

Fig. 4b. U.S. Real Output Growth, 1970:1 to 2020.

Philadelphia's Real-Time Data Set for Macroeconomists. The data comprise successive vintages from the National Income and Product Accounts, with each vintage reflecting the information available around the middle of the respective quarter. Croushore and Stark (2001) provide a description of the real-time GDP database. The GDP deflator price series used to measure inflation is constructed analogously. We define inflation (output growth) as the first difference in the logarithm of the GDP deflator (GDP) multiplied by 400.

Fig. 4a displays inflation, and (for context) Fig. 4b displays real output growth from 1970:1 to 2020:2 based on the final vintage of data.[17] Fig. 4c illustrates three well-known output gap measures, again based on the final vintage.

---

[17] The empirical analysis which follows uses a time sequence of vintages.

In Fig. 4a, during the Great Moderation, inflation typically exhibits lower volatility and lower conditional mean than for the 1970s and early 1980s. However, during the run up to the Great Recession, between 2003 and 2006, there are several realisations of high inflation. The upward spikes apparent during this period are often regarded as (the response to) relative price movements, and, in particular, commodity prices. See, for example, the analysis of Garratt and Petrella (2022). A striking feature of the Great Recession and its aftermath is the increased threat of low inflation, and an apparent increase in volatility. The recent pandemic resulted in a downward spike in inflation in early 2020.

3.2.3. Forecast combination and empirical transformation

The decision maker recursively combines the forecast densities from the experts. Each expert uses an expanding window for parameter estimation. For the first recursion, the estimation sample is 1970:1 to 1989:4 (window size,
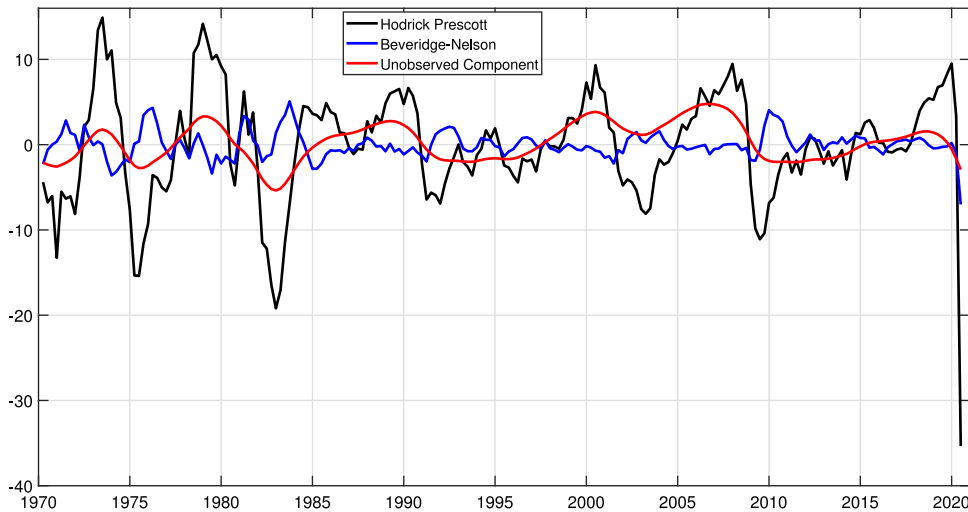
Fig. 4c. U.S. Output Gaps, 1970:1 to 2020.

80 observations) and the last 1970:1 to 2020:1 (window size, 201 observations).

As our U.S. GDP deflator data are released with a one-quarter lag, the first vintage, dated 1990:1, contains time series observations from 1970:1 to 1989:4, and the last vintage, dated 2020:4, has data from 1970:1 to 2020:3. Following Clark and McCracken (2010) and others, we use the second estimate as the target "final" data. For example, when evaluating the $h = 1$ forecast (nowcast) for 2020:2, we use the 2020:4 vintage observation of inflation for 2020:2.

Each VAR (expert) produces conditional forecast densities for inflation (and the (jth) output gap) through our evaluation period: $\tau = \underline{\tau}, \ldots, \overline{\tau}$ where $\underline{\tau} =$ 1990:1 and $\overline{\tau} =$ 2020:2 (122 quarterly observations). The point forecasts are the means of the conditional forecast densities.

To deploy EtLOP, the decision maker must fit a marginal distribution for inflation, π_t. Since the decision maker uses recursive fitting based on expanding windows of data, the fitted distributions for inflation vary by forecast origin in practice, but all appear non-Gaussian; see the earlier discussion of Figs. 2a and 2b.[18]

We emphasise that in this application, we follow the standard approach in the "real time" macroeconomic literature, fitting all models and the non-parametric margin to data vintages in the public domain at the forecast origin. We do not fit any parameters, or the ECDF of the target variable, on ex post data.

In the following section, we compare and contrast the forecast performance of EtLOP with the equal-weight benchmark LOP. The performance metrics used to gauge relative forecast accuracy include the RMSFE and sample-averaged CRPS, together with tail-weighted CRPS metrics.

3.2.4. Results

In this section, we report results for horizons one step ahead to four steps ahead. All results reported here use the equal-weight LOP as a benchmark.[19]

The second column of Table 1 reports the RMSFE, where the point forecasts are the means of the conditional distribution, and the third column reports the time-averaged CRPS over the evaluation sample. Columns 4 to 6 give the tail-weighted, right-tail-weighted, and left-tail-weighted CRPS, respectively. The values displayed in columns 2 to 6 are computed as ratios to the equal-weight benchmark LOP. Ratios less than one, for both RMSFE and CRPS, indicate an improvement in forecast performance relative to the equal-weight benchmark LOP.[20]

The RMSFEs reported in the second column indicate a gain for the EtLOP of approximately 13% over the benchmark for horizon $h = 1$, displayed in row 2. As the forecast horizon lengthens (rows 3 through 5), the performance gain from EtLOP increases monotonically to 34%. Similarly, the CRPS values reported in column 3 indicate a comparable performance gain from EtLOP, monotonically increasing from 14% at $h = 1$ (row 2) to 33% at $h = 4$ (row 5).

---

[18] As a rough guide, the null hypothesis of normality is rejected at the 1% significance level for all vintages, using the Shapiro–Wilk test.

[19] Recursive weighted combinations based on the sample-averaged logarithmic score and sample-averaged CRPS gave similar results.

[20] We compute the weighted or quantile CRPS using Eq. (17) in Gneiting and Ranjan (2011). Suppose the density forecast is f and π_τ is the realised inflation we use to evaluate the forecast. The quantile CRPS is defined as:

$$qwCRPS(f, \pi_\tau) = \frac{1}{K-1} \sum_{k=1}^{K-1} v(\alpha_k) QS_{\alpha_k}(F^{-1}(\alpha_k), \pi_\tau),$$

where

$$\alpha_k = \frac{k}{K}, \qquad K = 10{,}000.$$

$v(\alpha_k)$ is a non-negative quantile weight function on the unit interval ($\alpha \in (0, 1)$) that takes the values $(2\alpha - 1)^2$ when considering both tails,

Table 1
Forecast Evaluation for EtLOP.

Horizon	RMSFE	CRPS	TW	RTW	LTW
$h = 1$	0.867**	0.860**	0.850**	0.839**	0.877*
$h = 2$	0.802**	0.789**	0.774**	0.754**	0.828*
$h = 3$	0.734**	0.727**	0.726**	0.657**	0.814*
$h = 4$	0.660**	0.670**	0.696**	0.594**	0.751*

Notes: Columns 2 to 6 report ratios of EtLOP relative to the equal-weight benchmark LOP, for RMSFE, the CRPS, and the tail-weighted (TW), right-tail-weighted (RTW), and left-tail-weighted (LTW) CRPS statistics, respectively. Ratios less than one indicate an improvement in forecast performance relative to the benchmark. Improvements, using the two-sided test of Giacomini and White (2006) at the 1% and 5% significance levels are denoted ∗∗ and ∗, respectively.
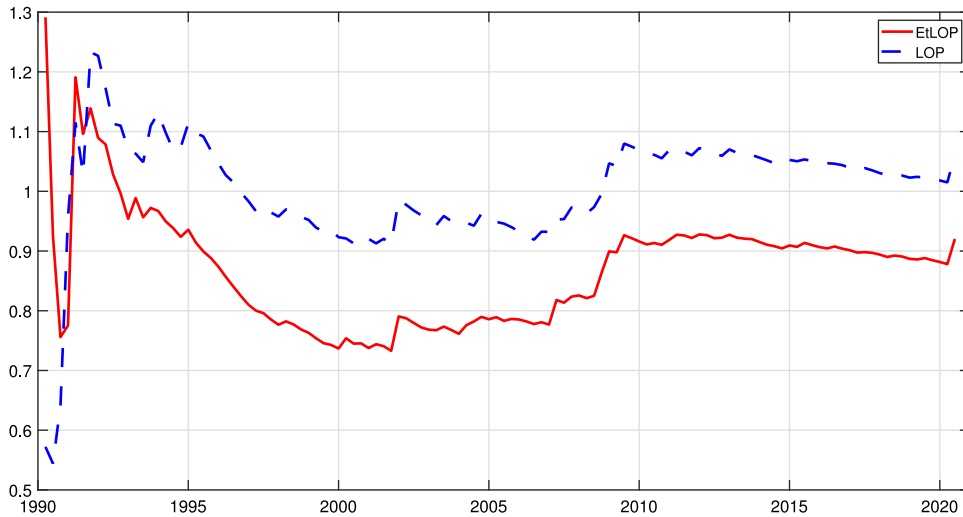
Fig. 5a. Recursive Forecast Performance, h=1, 1990:1 to 2020:2, RMSFE.
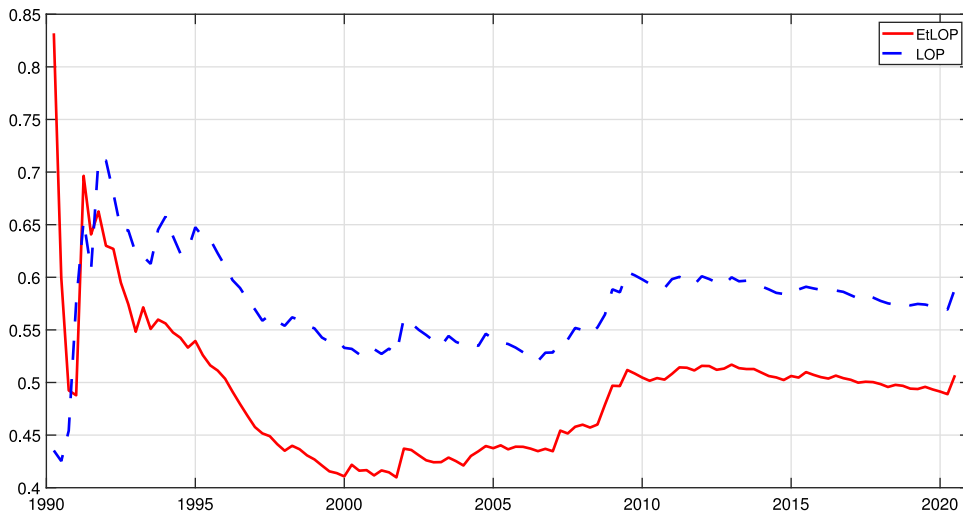
Fig. 5b. Recursive Forecast Performance, h=1, 1990:1 to 2020:2, Average CRPS.

Turning to the tail-weighted CRPS (columns 4 through 6), EtLOP performance is fairly consistent when considering both tails or just the right tail (columns 4 and 5),

whereas the left-tail-weighted CRPS results in a slightly smaller performance gain (column 6).

Figs. 5a and 5b display the relative forecasting performance differentials computed recursively, for the one step ahead case, $h = 1$, in terms of RMSFE and CRPS, respectively. Regardless of the forecast performance

---

α^2 for the right tail, and $(1 - \alpha)^2$ for the left tail. The quantile score, QS_{α_k}, uses the empirical distribution function F built from π_τ.
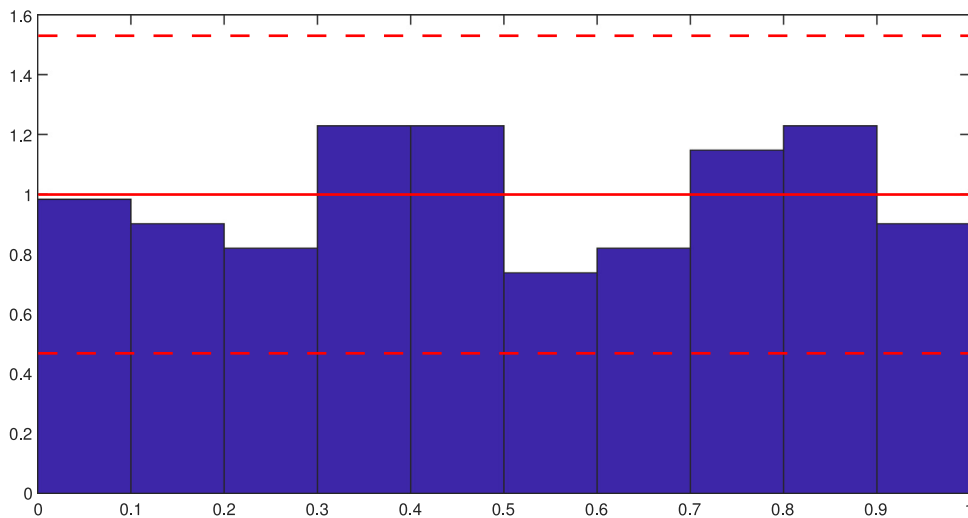
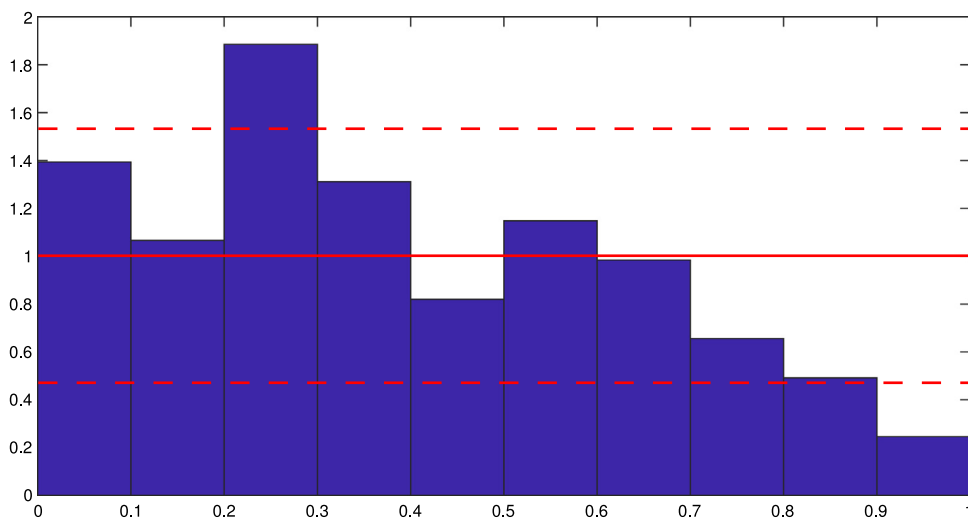**Fig. 6a.** PITs Histogram, h=1, 1990:1 to 2020:2, EtLOP.

Fig. 6b. PITs Histogram, h=1, 1990:1 to 2020:2, LOP.

metric, the EtLOP (red, solid line) dominates the equal-weight benchmark LOP (blue, dashed line) from 1992 onwards. The online appendix provides analysis for horizons 2 through 4; the plots display similar patterns.

To summarise the results so far, EtLOP outperformed the equal-weight benchmark LOP in terms of relative forecasting performance. To give further context, using the same metrics, EtLOP also outperformed the Bayesian estimated UCSV model and the BLOP at all horizons, as reported in the online appendix.

As a guide to absolute forecasting performance, Fig. 6a plots the (end-sample) histograms for the $h = 1$ PIT from EtLOP; whereas, Fig. 6b displays the corresponding histograms for the equal-weight benchmark LOP. Although close to uniform for EtLOP, the histograms for the benchmark have too many realisations in the left tail of the forecast density and too few in the right tail. The Kolmogorov–Smirnov-based calibration test of Rossi and

Sekhposyan (2019), for horizon $h = 1$, suggests that the null of "correct specification" cannot be rejected for EtLOP at the 10% significance level, with a test statistic of 0.546. However, the null is rejected easily at the 10% significance level for the benchmark, with a test statistic of 2.085.[21] Nevertheless, we stress that this is a short evaluation sample of 122 observations and that the combinations are misspecified by construction: the dependence between experts has been ignored in the combinations, consistent with the convention in the linear opinion pooling literature.

To provide further insight into EtLOP's relative forecast performance, focusing on the $h = 1$ case, Figs. 7a and 7b

---

21 The critical values, for $h = 1$, of the Kolmogrov–Smirnov RS test statistic are 1.61, 1.34, and 1.21 for the 1%, 5%, and 10% significance levels, respectively. Results using the Cramer–von Mises version of the Rossi and Sekhposyan (2019) test are similar. Results for $h = 4$ are also similar.
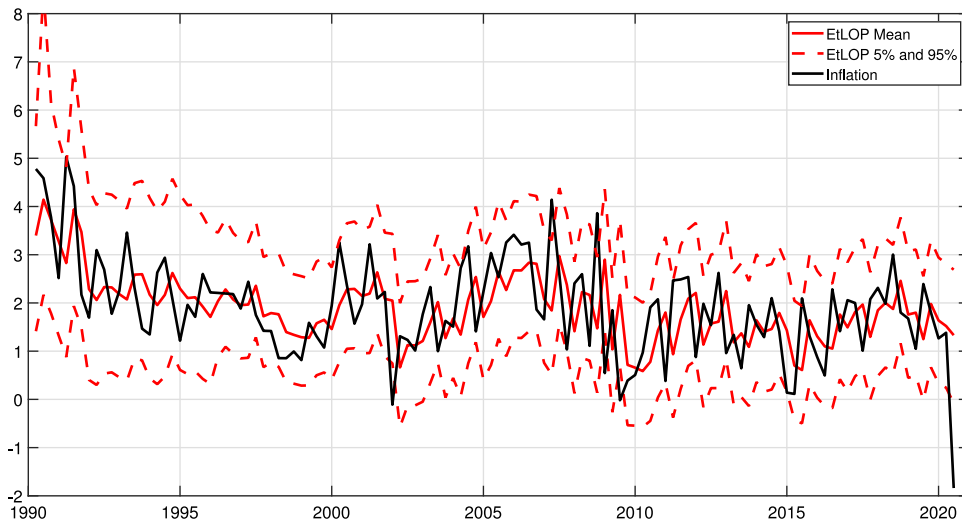
Fig. 7a. EtLOP Forecasts, h=1, 1990:1 to 2020:2.
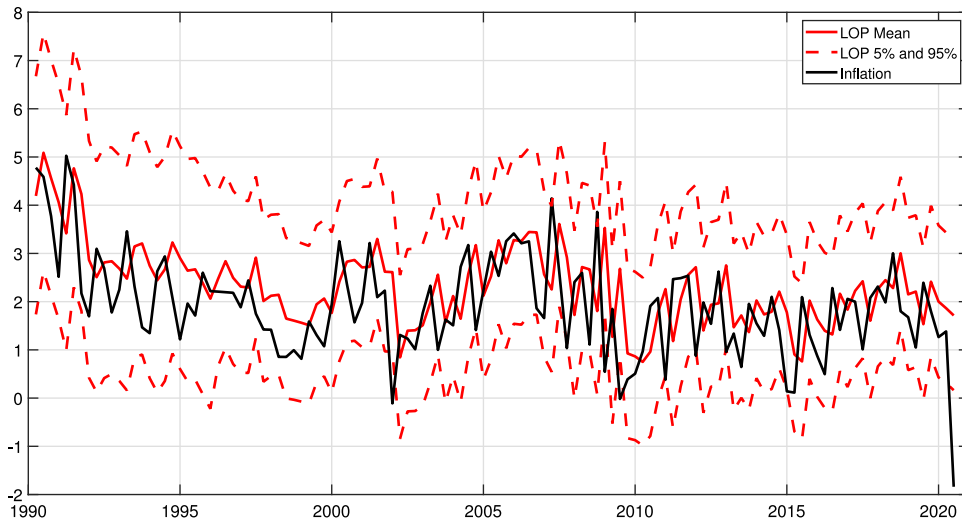

Fig. 7b. LOP Forecasts, h=1, 1990:1 to 2020:2.

display the 5th and 95th percentiles of the forecast densities, together with the conditional mean forecasts and inflation realisations, for the EtLOP and the benchmark, respectively. EtLOP's bands are narrower than the equal-weight LOP's for nearly all of the evaluation sample, with greater variation through time for EtLOP.

Fig. 8a through Fig. 8d complement Figs. 7a and 7b, displaying for $h = 1$ the differences between the 5th and 95th percentiles of the forecast density, a measure of skew, the p-value for skew, and the probability of inflation being less than 2.6%, respectively. Fig. 8a supports the assessment of Figs. 7a and 7b in that the EtLOP densities (red, solid line) are less diffuse than the equal-weight LOP densities (blue, dashed line). The EtLOP's densities display greater time variation, especially prior to 2000. Fig. 8b, which plots skew, reveals EtLOP to have positive skew for much of the evaluation, whereas the equal-weight

benchmark LOP has near zero skew throughout the evaluation sample. The p-values displayed in Fig. 8c confirm the significance of EtLOP's skew from 1990 to 2005, but with a drop in the *p*-value thereafter. Fig. 8d reveals that the EtLOP assigns a higher probability than the LOP to the event of inflation being less than the unconditional mean, 2.6%, throughout the evaluation sample. The EtLOP implies higher risk of below-mean inflation events. The online appendix provides corresponding plots to Fig. 8a through Fig. 8d but for horizons $h = 2$ through $h = 4$. The results are similar to the $h = 1$ case, except that there is more significant skew towards the end of the sample at longer horizons with EtLOP.

In summary, the plots in Figs. 7 and Fig. 8 reveal that the EtLOP forecast densities have skew, whereas the equal-weight benchmark LOP forecast densities are approximately symmetric. Furthermore, EtLOP forecast
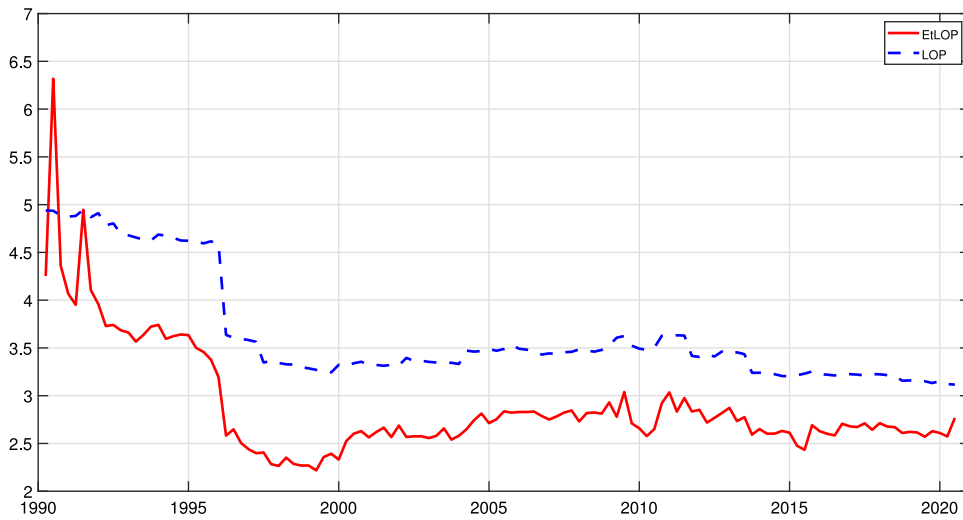
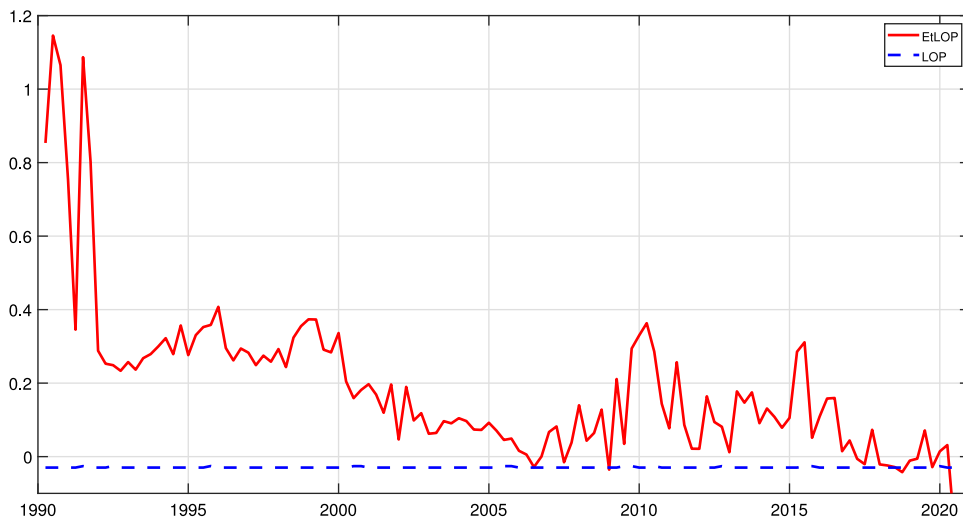**Fig. 8a.** Uncertainty Range (95%-5%)

Fig. 8b. Skew.

densities are less diffuse, with more variation in the diffusion through time.

Finally, Figs. 9a–9d display the forecast densities for EtLOP (red, solid line) and the equal-weight benchmark LOP (blue, dashed line) for the target observations of 2009:1 through to 2009:4, when inflation was unusually low. The EtLOP densities have less probability mass on high inflation and are somewhat less diffuse than their conventional counterparts. The EtLOP displays some asymmetry for these notable observations, but the skew is not particularly strong.

4. Conclusions

In this paper, we proposed a methodology to improve the accuracy of the LOP. Our approach involves transforming the conventional combination forecast densities using an ECDF to match the distribution of the sample data. In

our U.S. inflation application, we combined forecast densities from a system of VAR models. We demonstrated that the empirically transformed LOP considerably improved forecasting performance relative to the more conventional equal-weight opinion pool.

Declaration of competing interest

The authors declare that they have no known competing financial interests or personal relationships that could have appeared to influence the work reported in this paper.

Appendix A. Output trend definitions

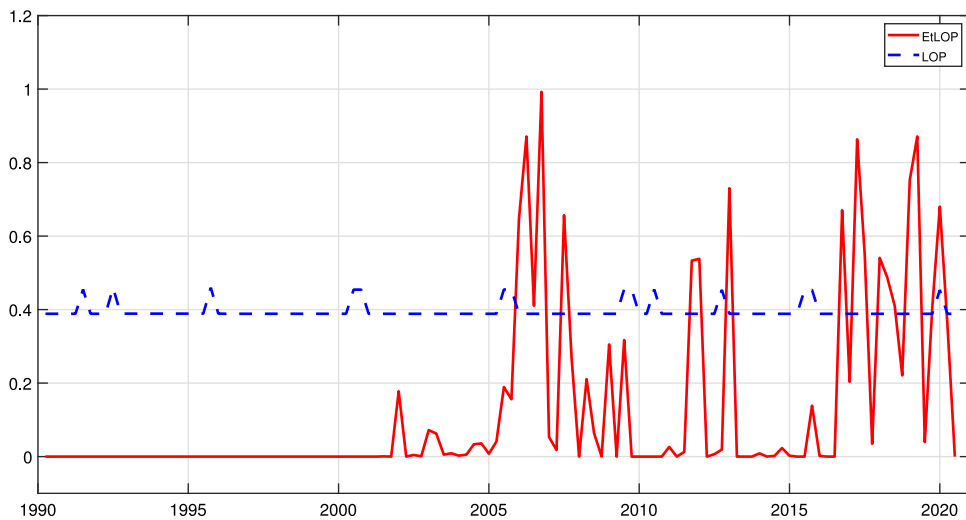We summarise the seven univariate detrending specifications below.
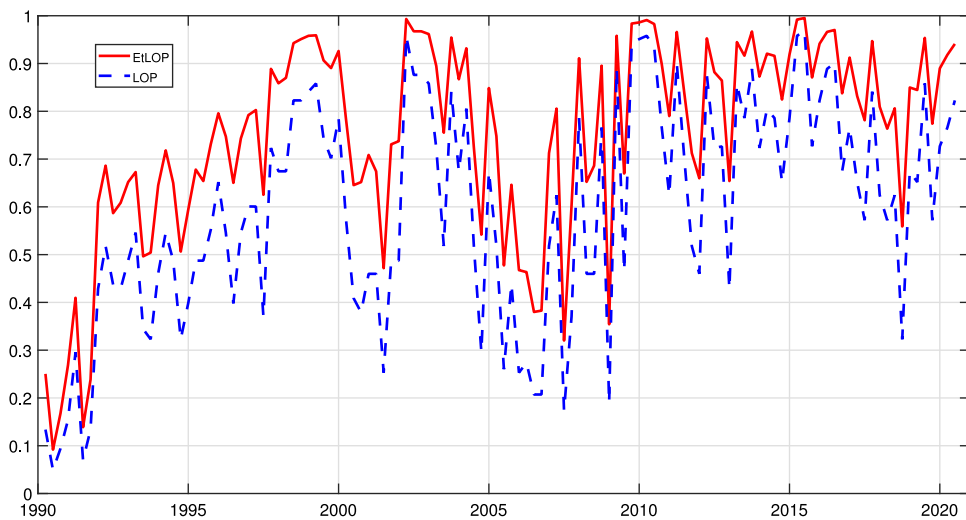
Fig. 8c. P-value Skew.

Fig. 8d. Pr(Inflation < 2.6%)

1. For the quadratic trend-based measure of the output gap we use the residuals from a regression (estimated recursively) of output on a constant and a squared time trend.
2. Following Hodrick and Prescott (1997, HP), we set the smoothing parameter to 1600 for our quarterly U.S. data.[22]
3. Since the HP filter is a two-sided filter, it relates the time-t value of the trend to future and past observations. Moving towards the end of a finite sample of data, the HP filter becomes progressively one-sided and its properties deteriorate with the mean squared error (MSE) of the unobserved components increasing and the estimates ceasing to

be optimal in an MSE sense. We therefore follow Mise et al. (2005) and mitigate this loss near and at the end of the sample by extending the series with forecasts. At each recursion the HP filter is applied to a forecast-augmented output series (again with smoothing parameter 1600), with forecasts generated from a univariate AR(8) model in output growth (again estimated recursively using the appropriate vintage of data). The implementation of forecast augmentation when constructing real-time output gap measures for the U.S. is discussed at length in Garratt et al. (2008). We deliberately select a high lag order to ensure that no important lags are omitted—favouring unbiasedness over efficiency.

4. Christiano and Fitzgerald (2003) propose an optimal finite-sample approximation to the band-pass filter, without explicit modelling of the data. Their
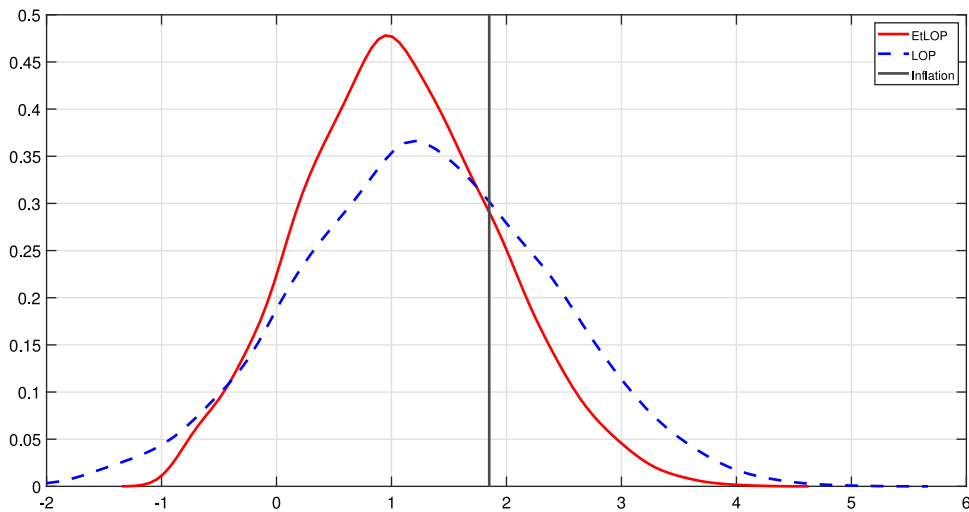
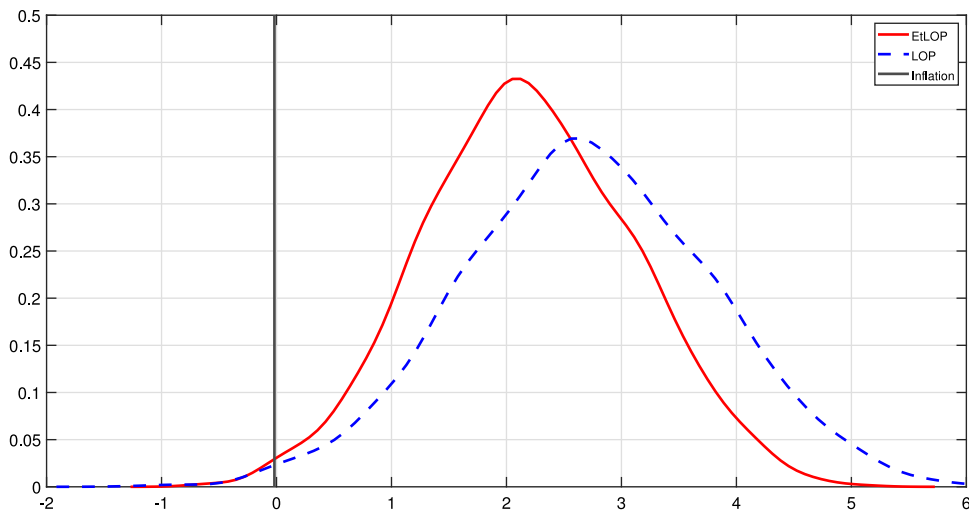**Fig. 9a.** Forecast Densities for 2009:1, h = 1.

Fig. 9b. Forecast Densities for 2009:2, h=1.

approach implicitly assumes that the series is captured reasonably well by a random walk model and that, if there is drift present, this can be proxied by the average growth rate over the sample.

5. We also consider the band-pass filter suggested by Baxter and King (1999). We define the cyclical component to be fluctuations lasting no fewer than six and no more than 32 quarters—the business cycle frequencies indicated by Baxter and King (1999)—and set the truncation parameter (the maximum lag length) at three years. As with the HP filter we augment our sample with AR(8) forecasts to fill in the "lost" output gap observations at the end of the sample due to truncation.

6. The Beveridge and Nelson (1981) decomposition relies on a priori assumptions about the correlation between permanent and transitory innovations. The approach imposes the restriction that shocks to the transitory component and shocks to the stochastic permanent component have a unit correlation. We assume that the ARIMA process for output growth is an AR(8), the same as that used in our forecast augmentation.

7. Finally, our unobserved components model assumes that q_t is decomposed into trend, cyclical, and irregular components:

$$q_t = \mu_t^7 + \psi_t^7 + \xi_t, \quad \xi_t \sim i.i.d. \ N(0, \sigma_\xi^2), \quad t = 1, \dots, T$$

(A.1)

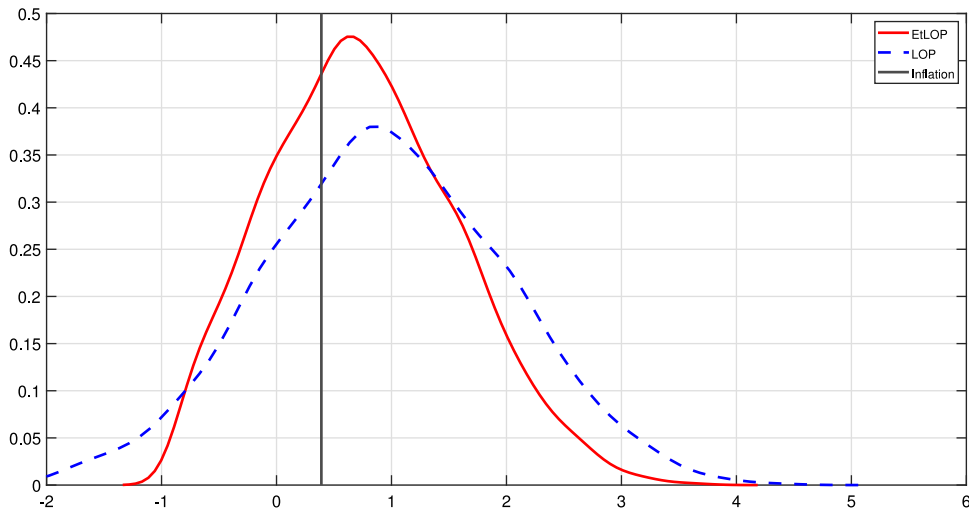where the stochastic trend is specified as

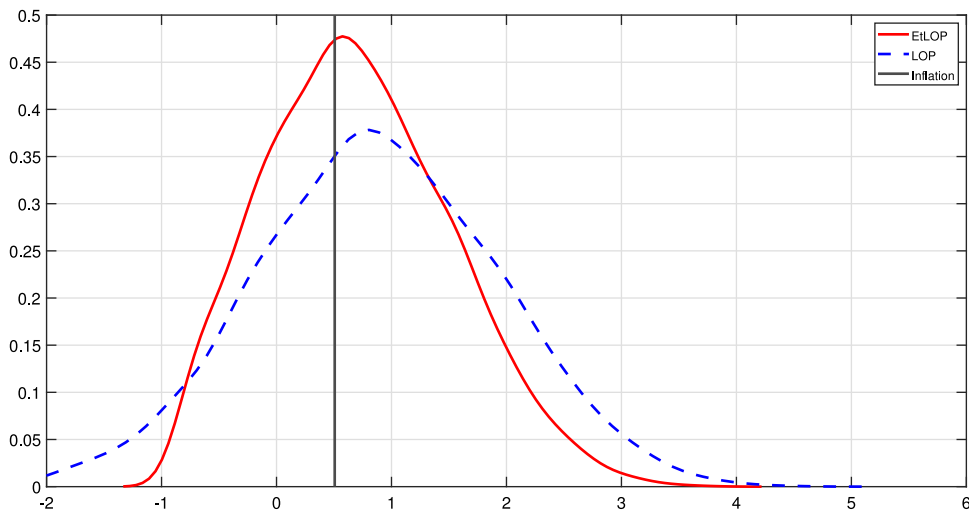**Fig. 9c.** Forecast Densities for 2009:3, h=1.

Fig. 9d. Forecast Densities for 2009:4, h=1.

$$\mu_t^7 = \mu_{t-1}^7 + \beta_{t-1} + \eta_t, \quad \eta_t \sim i.i.d. \ N(0, \sigma_\eta^2)$$

$$\beta_t = \beta_{t-1} + \zeta_t, \quad \zeta_t \sim i.i.d. \ N(0, \sigma_\zeta^2).$$

Letting $\sigma_\zeta^2 > 0$ but setting $\sigma_\eta^2 = 0$, gives an integrated random walk. The cyclical component is assumed to follow a stochastic trigonometric process:

$$\begin{bmatrix} \psi_t^7 \\ \psi_t^{7*} \end{bmatrix} = \rho \begin{bmatrix} \cos\lambda & \sin\lambda \\ -\sin\lambda & \cos\lambda \end{bmatrix} \begin{bmatrix} \psi_{t-1}^7 \\ \psi_{t-1}^{7*} \end{bmatrix} + \begin{bmatrix} \kappa_t \\ \kappa_t^* \end{bmatrix}$$

(A.2)

where λ is the frequency in radians, ρ is a damping factor, and κ_t and κ_t^* are two independent white noise Gaussian disturbances with common variance σ_κ^2. We estimate this model by maximum likelihood, exploiting the Kalman filter, and estimates of the trend and cyclical components are obtained using the Kalman smoother.

Appendix B. Supplementary data

Supplementary material related to this article can be found online at https://doi.org/10.1016/j.ijforecast.2022.02.003.

References

Aastveit, K. A., Mitchell, F., Ravazzolo, J., & van Dijk, H. K. (2019). The evolution of forecast density combinations in economics. In *Oxford research encyclopedia of economics and finance*. Oxford University Press.

Adrian, T., Boyarchenko, D., & Giannone, N. (2019). Vulnerable growth. *American Economic Review, 109*(4), 1263–1289.

Adrian, T., Boyarchenko, D., & Giannone, N. (2021). Multimodality in macrofinancial dynamics. *International Economic Review, 62*(2), 861–886.

Allayioti, A. (2020). *Bayesian entropic tilting for macroeconomic variables with reshaped survey information*. mimeo: Warwick Business School, University of Warwick.

Amengual, D., Sentana, Z., & Tian, E. (2020). *Gaussian rank correlation and regression*: CEPR discussion papers 14914, June.

Bassetti, F., Casarin, F., & Ravazzolo, R. (2018). Bayesian nonparametric calibration and combination of predictive distributions. *Journal of the American Statistical Association*, *113*(552), 675–685.

Baxter, M., & King, R. G. (1999). Measuring business cycles: Approximate band-pass filters for economic time series. *The Review of Economics and Statistics*, *81*, 594–607.

Beveridge, S., & Nelson, C. R. (1981). A new approach to decomposition of time series into permanent and transitory components with particular attention to measurements of the business cycle. *Journal of Monetary Economics*, 7, 151–174.

Carriero, A., Clark, M., & Marcellino, T. E. (2020). *Capturing macroeconomic tail risks with bayesian vector autoregressions*: *Working paper No. 20-02, January*, Federal Reserve Bank of Cleveland.

Christiano, L., & Fitzgerald, T. J. (2003). The band pass filter. *International Economic Review*, *44*(2), 435–465.

Clark, T. E., & McCracken, M. W. (2010). Averaging forecasts from VARs with uncertain instabilities. *Journal of Applied Econometrics*, January-February, 5-29.

Coe, P. J., & Vahey, S. P. (2020). *Financial conditions and the risks to economic growth in the united states since 1875*: *CAMA working paper No. 36/2020*, Australian National University, April.

Cogley, Timothy, Morozov, Sergei, & Sargent, Thomas J. (2005). Bayesian fan charts for U.K. inflation: Forecasting and sources of uncertainty in an evolving monetary system. *J. Econ. Dyn. Control*, *29*(11), 1893–1925.

Croushore, D., & Stark, T. (2001). A real-time data set for macroeconomists. *Journal of Econometrics*, *105*, 111–130.

DeGroot, M. H., & Mortera, J. (1991). Optimal linear opinion pools. *Management Science*, *37*(5), 546–558.

Deheuvels, P. (1979). La Fonction de Dépendance Empirique et Ses Propriétés. Un Test non Paramétrique d'Indépendance. *Bulletin Royal Belge de L'Académie Des Sciences*, *65*, 274–292.

Deheuvels, P. (1981). An asymptotic decomposition for multivariate distribution-free tests of independence. *Journal of Multivariate Analysis*, *11*(1), 102–113.

Diebold, F. X., Gunther, A. S., & Tay, T. A. (1998). Evaluating forecast densities; with applications to financial risk management. *International Economic Review*, *39*, 863–883.

Diebold, F. X., & Shin, M. (2019). Machine learning for regularized survey forecast combination: Partially-egalitarian lasso and its derivatives. *International Journal of Forecasting*, *35*(4), 1679–1691.

Diebold, F. X., Shin, B., & Zhang, M. (2021). *On the aggregation of probability assessments: regularized mixtures of predictive densities for Eurozone inflation and real interest rates*. Penn Institute for Economic Research, 21-002, January.

Galbraith, J. W., & van Norden, S. (2012). Assessing gross domestic product and inflation probability forecasts derived from bank of England fan charts. *Journal of the Royal Statistical Society, Series A (Statistics in Society)*, *175*(3), 713–727.

Galvao, A. B., Garratt, J., & Mitchell, A. (2021). Does judgement improve macroeconomic forecast densities? *International Journal of Forecasting*, *37*(3), 1247–1260.

Ganics, G. (2017). *Optimal density forecast combinations*: *Bank of spain working paper*, (1751).

Garratt, A., Lee, E., Mise, K., & Shields, K. (2008). Real-time representations of the output gap. *The Review of Economics and Statistics*, *90*(4), 792–804.

Garratt, A., Mitchell, J., & Vahey, S. P. (2014). Measuring output gap nowcast uncertainty. *International Journal of Forecasting*, *30*(2), 268–279.

Garratt, A., Mitchell, S. P., Vahey, E., & Wakerly, J. (2011). Real-time inflation forecast densities from ensemble phillips curves. *North American Journal of Economics and Finance*, *22*, 77–87.

Garratt, A., & Petrella, I. (2022). Commodity prices and inflation risk. *Journal of Applied Econometrics*, (Forthcoming in 2022).

Geweke, J., & Amisano, G. (2011). Optimal prediction pools. *Journal of Econometrics*, *164*, 130–141.

Giacomini, R., & White, H. (2006). Tests of conditional predictive ability. *Econometrica*, *74*, 1545–1578.

Gneiting, T., & Ranjan, R. (2011). Comparing forecast densities using threshold- and quantile-weighted scoring rules. *Journal of Business & Economic Statistics*, *29*(3), 411–422.

Gneiting, T., & Ranjan, R. (2013). Combining predictive distributions. *Electronic Journal of Statistics*, *7*, 747–1782.

Hodrick, R., & Prescott, E. (1997). Post-war U.S. business cycles: An empirical investigation. *Journal of Money, Banking and Credit*, *29*, 1–16.

Jore, A. S., Mitchell, S. P., & Vahey, J. (2010). Combining forecast densities from VARs with uncertain instabilities. *Journal of Applied Econometrics*, *25*, 621–634.

Karagedikli, O., Vahey, E. C., & Wakerly, S. P. (2019). *Improved methods for combining point forecasts for an asymmetrically distributed variable*: *CAMA working paper No. 15/2019*, Australian National University, February.

Kascha, C., & Ravazzolo, F. (2010). Combining inflation forecast densities. *Journal of Forecasting*, *29*, 231–250.

Knüppel, M., & Krüger, F. (2022). Forecast uncertainty, disagreement, and the linear pool. *Journal of Applied Econometrics*, *37*(1), 23–41.

Loaiza-Maya, R., & Smith, M. S. (2020). Real-time macroeconomic forecasting with a heteroskedastic inversion copula. *Journal of Business & Economic Statistics*, *38*(2), 470–486.

Mise, E., Kim, P., & Newbold, T.-H. (2005). On the sub-optimality of the hodrick–prescott filter. *Journal of Macroeconomics*, *27*(1), 53–67.

Odendahl, F. (2018). *Survey-based joint forecast densities*. mimeo: UPF, October.

Orphanides, A., & van Norden, S. (2002). The unreliability of output-gap estimates in real time. *The Review of Economics and Statistics*, *84*(4), 569–583.

Orphanides, A., & van Norden, S. (2005). The reliability of inflation forecasts based on output-gap estimates in real time. *Journal of Money Credit and Banking*, *37*(3), 583–601.

Ranjan, R., & Gneiting, T. (2010). Combining probability forecasts. *Journal of the Royal Statistical Society. Series B.*, *72*, 71–91.

Rosenblatt, M. (1952). Remarks on a multivariate transformation. *The Annals of Mathematical Statistics*, *23*, 470–472.

Rossi, B. (2019). *Forecasting in the presence of instabilities: how do we know whether models predict well and how to improve them*: *Barcelona GSE working paper series working paper 1161*, November.

Rossi, B., & Sekhposyan, T. (2014). Evaluating predictive densities of U.S. output growth and inflation in a large macroeconomic data set. *International Journal of Forecasting*, *30*(3), 662–682.

Rossi, B., & Sekhposyan, T. (2019). Alternative tests for correct specification of conditional predictive densities. *Journal of Econometrics*, *208*(2), 638–657.

Shimazaki, H., & Shinomoto, S. (2010). Kernel bandwidth optimization in spike rate estimation. *Journal of Computational Neuroscience*, *29*, 171–182.

Smith, M. S., & Vahey, S. P. (2016). Asymmetric forecast densities for U.S. macroeconomic variables from a Gaussian copula model of cross-sectional and serial dependence. *Journal of Business & Economic Statistics*, *34*, 416–434.

Timmermann, A. (2006). Forecast combinations. In *Handbook of economic forecasting* (pp. 135–196).

Velásquez-Giraldo, M., Canavire-Bacarreza, G., Huynh, K., & Jacho-Chavez, D. T. (2018). Flexible estimation of demand systems: A copula approach. *Journal of Applied Econometrics*, *33*, 1109–1116.